INTERNATIONAL JOURNAL OF CIVIL ENGINEERING AND TECHNOLOGY (IJCIET)

ISSN 0976 – 6308 (Print)
ISSN 0976 – 6316(Online)
Volume 5, Issue 11, November (2014), pp. 125-145

Journal Impact Factor (2014): 7.9290 (Calculated by GISI)
www.jifactor.com

IJCIET

©IAEME

STRENGTH AND BEHAVIOR OF INNOVATIVE COMPOSITE COLUMNS

Y. B. shaheen[1], R.M. Abd El-Naby[2], M.A. Adam[3], A.M. Erfan[4]

[1]Professor, Civil Eng. Dep., Faculty of Eng., Monfiya University, Egypt
[2]Professor, Civil Eng. Dep., Shoubra Faculty of Eng., Benha University, Egypt
[3]Associate Professor, Civil Eng. Dep., Shoubra Faculty of Eng., Benha University, Egypt
[4]Assistant Lecture, Civil Eng. Dep., Shoubra Faculty of Eng., Benha University, Egypt

ABSTRACT

This paper presents a proposed method for producing reinforced composite concrete columns reinforced with various types of wire meshes. The experimental program includes casting and testing of eighteen square columns having the dimensions of 150 mm x150 mm x1500mm under concentric compression loadings. The test samples comprise five designation series to make comparative study between conventionally reinforced concrete columns and concrete columns reinforced with welded steel mesh expanded steel mesh, fiber glass mesh and tensar mesh. The main variables are the type of innovative reinforcing materials, metallic or non metallic, the number of layers and volume fraction of reinforcement. The main objective is to evaluate the effectiveness of employing the new innovative materials in reinforcing the composite concrete columns. The results of an experimental investigation to examine the effectiveness of these produced columns are reported and discussed including strength, deformation, cracking, ductility and energy absorption properties. The results proved that new reinforced concrete columns can be developed with high strength, crack resistance, high ductility and energy absorption properties using the innovative composite materials. Also, Non-linear finite element analysis; (NLFEA) was carried out to simulate the behaviour of the reinforced concrete composite columns. The numerical model could agree the behaviour to satisfy level with test results employing ANSYS-9.0 Software.

Keywords: Ferro-Cement; Expanded Steel Mesh; Fiber Glass Mesh; Welded Steel Mesh Steel Mesh; Polypropylene Mesh; Polypropylene Fiber; Deformation Characteristics; Strength; Cracking; Ductility; Energy Absorption.

International Journal of Civil Engineering and Technology (IJCIET), ISSN 0976 – 6308 (Print), ISSN 0976 – 6316(Online), Volume 5, Issue 11, November (2014), pp. 125-145 © IAEME

1. INTRODUCTION

Ferro-cement can be defined as a thin wall reinforced concrete commonly constructed of hydraulic cement mortar reinforced with closely spaced layers of continuous and relatively small diameter wire mesh. Ferro-cement is ideally suited for structures in which predominant membrane stresses occur. As a result, it has been extensively used to construct different element such as, tanks, roofs, bridge decks…etc. For reinforced concrete structures, the column is the most important and critical element that can determine the behavior and failure mode of the structure. In the last few decades, incidence of failures of reinforced concrete structures has been seen widely because of increasing service loads, seismic loads and/or durability problems. The economic losses due to such failures are billions of dollars. Mansur and Paramasivan (1990) carried out an experimental investigation on ferro-cement box-section short columns with and without concrete infill under axial and eccentric compression. The studied parameters were the types, arrangements, and volume fraction of reinforcement. Test results indicated that a ferro-cement box- section can be used as a structural column. Welded wire mesh has been found to perform better than an equivalent amount of woven mesh. Another interesting research was done by Ahmed et al. (1994) to investigate the possibility of using ferro-cement as a retrofit material for masonry columns. Uniaxial compression tests were performed on three uncoated brick columns, six coated brick columns with 25 mm plaster and another six columns coated with 25 mm thick layer of ferro-cement. The study demonstrated that the use ferro-cement coating strengthens brick columns significantly and improves their cracking resistance. Kaushik et al. (1994) carried out an investigation for ferro-cement encased concrete columns. They have investigated short circular as well as square columns with unreinforced and reinforced cores. It was seen that the ferro-cement encasement increases the strength and ductility of the columns for both axial and eccentric loading conditions. Nedwell et al. (1994) conducted a preliminary investigation into the repair of short square columns using ferro-cement. Also, several investigations have been reported on different ferro-cement elements under axial load and eccentric compression by Fahmey, E, Shaheen, Korany, Y.S. in (2004) and Fahmey, E, Shaheen, Abou Zeid, M.N., Gaafar, H. (2005). Abdel Tawab, Alaa, (2006) investigated the use of U-shaped ferro-cement permanent forms for the construction of beams and Hazem, R.(2009), used non-metallic reinforcement for the U-shaped ferro-cement forms instead of the conventional steel mesh. Applying the ferro-cement concept in construction of concrete beams incorporating reinforced mortar permanent forms is investigated by Fahmy *et al*. (2013). This paper presents the results of an investigation aimed at developing reinforced concrete beams consisting of pre-cast permanent U-shaped reinforced mortar forms filled with different types of core materials to be used as a viable alternative to the conventional reinforced concrete beam. A short program was undertaken to provide some information regarding the effect of ferro-cement repair on short columns subjected to axial loadings. It was found that the use of ferro-cement retrofit coating increases the apparent stiffness of the columns and significantly improves the ultimate load carrying capacity.

Due to the importance of column as a main element in the concrete structures, there is still need to develop and investigate new materials used in column casting to improve its behavior till failure. Using innovative composites will satisfy some of column needs to enhance its behavior and increase strength, ductility and energy absorption.

2. EXPERIMENTAL PROGRAM AND TEST SETUP

Eighteen composite columns having the cross section dimensions of 150 mm x150 mm with 1500 mm long were casted as shown in Fig. 1 and Table 1. The concrete mix for the test specimens was designed to obtain compressive strength 50 MPa at 28 days age. The mix proportions were 2 sand: 1 cement, water cement ratio was 0.35 and 1.5% super plasticizer by weight of cement. Various

types of reinforcing materials were employed as shown in Fig. 2. All specimens were tested under axial compression loadings. By using Compression Testing Machine with capacity of 5000 KN as shown in Fig. 3. The test work was performed at the Reinforced Concrete Laboratory of Housing and Building National Research Centre (HBNRC) at Giza, Egypt. The main components of the testing facility are: Control Station, Loading Cells and Testing Frame. The load was applied via loading cell which was acting at the column head. The load was incrementally applied with an increment of 5.0 to 20 KN for all the test specimens as shown in Fig. 3.

Table: 1: Specification of tested specimens

Series	Specimen NO.	Description	Volume fraction %
Control Specimen	C1	Control specimen reinforced by 4Φ12 longitudinal bars and 11 Φ6 stirrups	2.564
Series A		Expanded wire mesh	
	C1-A	one layer Expanded +4Φ12 + 6 Φ 6 stirrups.	2.681
	C2-A	two layers Expanded +4Φ12 + 6 Φ 6 stirrups	3.048
	C3-A	three layers Expanded +4Φ12 without stirrups	3.115
	C4-A	one layer Expanded +4Φ12 without stirrups	2.390
Series B		Welded wire mesh	
	C1-B	one layer welded +4Φ12 + 11 Φ 6 stirrups	2.685
	C2-B	two layers welded +4Φ12 + 6 Φ 6 stirrups	2.556
	C3-B	one layer welded +4Φ12 + 6 Φ 6 stirrups	2.434
	C4-B	two layers welded +4Φ12 without stirrups	2.254
	C5-B	three layers welded +4Φ12 without stirrups	2.376
	C6-B	four welded layers +4Φ12 without stirrups	2.498
Series C		Fiber glass mesh (F.G.)	
	C1-C	one layer F.G.+ one Gavazia mesh +4Φ12 + 6 Φ 6 stirrups	3.055
	C2-C	two layers F.G. mesh + 4Φ12 + 6 Φ 6 stirrups	2.726
	C3-C	three layers F.G. mesh + 4Φ12 + 6 Φ 6 stirrups	2.933
Series D	C1-D	Expanded wire mesh + Welded wire mesh One layer Expanded layer +one Welded layer + 4Φ12 + 6 Φ 6 stirrups	2.802
	C2-D	two layers Expanded layer +one Welded layer+ 4Φ12 + 6 Φ 6 stirrups	3.170
Series E		Tensar mesh	
	C1-E	One layer Tensar mesh layer + 4Φ12 + 11 Φ 6 stirrups	3.029
	C2-E	One layer Tensar mesh layer+ 4Φ12 + 6 Φ 6 stirrups	2.778

3. TEST RESULTS AND DISCUSSION

In what follows the performance of the reinforced concrete columns reinforced with different innovative composite materials is presented and discussed. The compression strength behaviour was investigated including the load-carrying capacity, the cracking pattern, the failure mode and finally the specimen's deformation and strains.

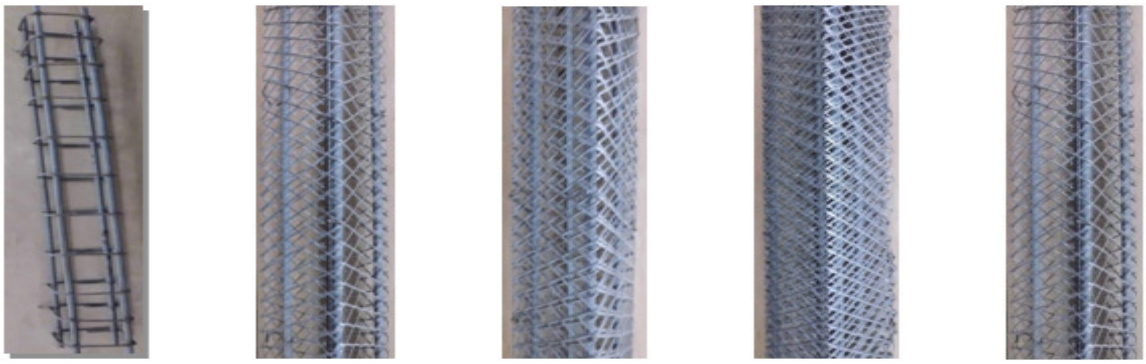

1) C1 2) C1-A 3) C2-A 4) C3-A 5) C4-A

Fig.1.a: Experimental specimens of control specimen reinforced and series A

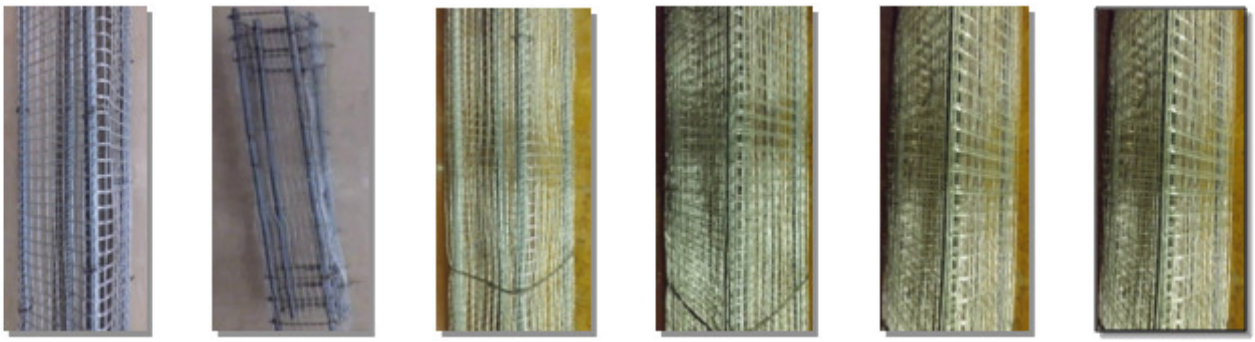

1) C1-B 2) C2-B 3) C3-B 4) C4-B 5) C5-B 6) C6-B

Fig.1.b: Experimental specimens of series B

a) C1-C b) C2-C c) C3-C

Fig. 1.c: Experimental specimens of series C

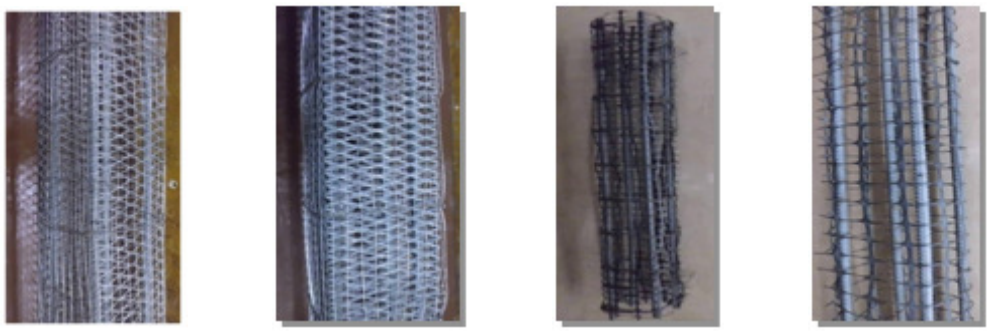

1) C1-D 2) C2-D 3) C1-E 4) C2-E

Fig. 1.d: Experimental specimens of series D and E

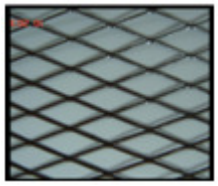

a) Expanded Wire mesh

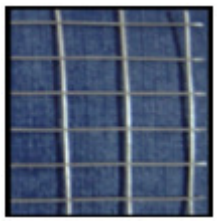

b) Welded Wire Mesh

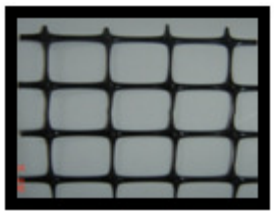

c) Polyethylene(Tensar)mesh

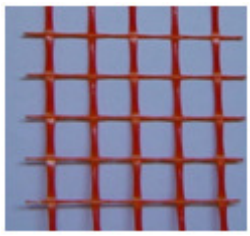

d) Fiber glass mesh

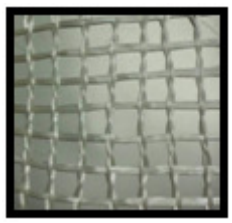

e) Gavazia mesh

f) Fibermesh 300

Fig. 2: Configurations of composites materials

Fig. 3: Test setup and data logger used in recording results

3.1 Ultimate Capacity

The failure load of the control specimen; C1 is shown in table 2 was 723.85 KN. For specimen C1-A, the failure load was 840.4 KN indicating significant enhancement in the ultimate capacity. The enhancement in the load-carrying capacity was 16.1 %. For specimens reinforced with two layers of expanded mesh and six stirrups only C2-A the increase in the ultimate capacity reached 21.5 %. For the specimen C3-A which reinforced with three layers of expanded wire mesh without stirrups the failure load was 951.82 KN with an enhancement of 31.4% this is due to using the expanded layers. For the specimen reinforced with two layers of expanded wire mesh without stirrups, C4-A the experimental failure load was 800 KN with an increase of 10.5%.

For series B that reinforced with welded wire mesh, the first specimen in this group was C1-B which reinforced with one welded mesh and eleven stirrups, the failure load was 743.2 KN with a relatively small enhancement of 2.7%. For C2-B the specimen reinforced with two welded wire mesh and six stirrups, the failure load was 800 KN with an increase of 10.5%. For the specimen reinforced with one welded wire mesh and six stirrups C3-B, the failure load was 776.66 KN with an

increase of 7.3%. For C4-B which reinforced with two welded wire mesh without stirrups the failure load was 780 KN with an enhancement of 7.7%. For C5-B reinforced with three welded wire mesh without stirrups the failure load was 833 KN with an enhancement of 15.1%. For C6-B which reinforced with four welded wire mesh without stirrups the failure load was 867 KN with an enhancement of 19.8%. According to the results in table **2** the effect of using expanded wire mesh is more effective than the welded wire mesh.

For series C reinforced with glass fibre reinforced polymers, the specimen C1-C reinforced with one layer of gavazia mesh and six stirrups the failure failed at 780 KN with an enhancement of 7.7%. The specimen reinforced with two layers of glass fibre and six stirrups C2-C, failed at load of 725 KN with almost no increase in loading with respect to the control specimen. The failure load increased by 2.5% to be 741.88 KN for specimen C3-C which reinforced using three layers of glass fibre and six stirrups. These results show the weakness of glass fibre in confinement with respect to other types used in this research. However this technique is good for resistance of corrosion and the long observed descending part in load displacement curve indicates the ability of this technique to be used under dynamic and earthquake effects.

For the series D which reinforced with welded and expanded wire meshes, the first specimen C1-D reinforced with one layer of welded mesh and one layer of expanded mesh and six stirrups, the failure load was 839.77 KN with an enhancement of 16.0% . For specimen C2-D the reinforced with one layer welded wire mesh and two layers expanded wire meshes and six stirrups, the failure load was 890 KN with an increase of 22.9%. For the series E reinforced with tensar, the specimen C1-E reinforced with one layer of tensar mesh and eleven stirrups the failure load was 787.5 KN with an enhancement of 8.7% but for C2-E which reinforced using one layer of tensar mesh and six stirrups the failure load is increased to be more than the control specimen by 1.3% to be 732.87 KN as shown in table **2**. Figure 4 through figure 8 shows the comparisons between load displacement curves of the tested specimens for each series. Also, Fig.9 indicates the enhancement percentage in experimental carrying load capacity for different specimens.

3.2 Cracking

The first cracks in control specimen started at load of 400 KN at the column head under the point of load concentration, and then propagated suddenly at the maximum load of 723.85 KN. After this, the load decreases and the cracks increased showing the failure of column. For specimens of series A, the recorded first crack load showed increased about 60%, 67%, 73%, 50%, for specimens C1-A, C2-A, C3-A and C4-A respectively. For specimens of series B which were C1-B, C2-B, C3-B, C4-B, C5-B and C6-B cracks loads were recorded to show an increase of 37%, 40%, 15%, 12%, 22% and 26% with respect to the control specimen respectively. For specimens of series C, C1-C, C2-C, and C3-C lower values of cracking load were observed with respect to the other specimens to be 22%, 20% and 21% larger than those of control specimen. For specimens of series D, C1-D and C2-D higher cracking load being 47% and 50% higher than the control specimen. For specimens C1-E and C2-E of series E, the first crack load recorded lower cracks load with respect to the control specimen being 98% and 93% of it respectively. This indicates the weakness of the tensar than the other techniques.

Generally, the cracks for all tested columns started at later stage of loading indicating better confinement and better serviceability. However, different types of innovative composite the ultimate strength increased and the cracks slightly increased in length and width to different extent. As shown in Figures 10 and Fig. 11 and table 3.

Mode of Failure

Near failure, the control specimen column failed in a mode of compression failure accompanied with local crushing and spalling of the concrete cover. For the other series of the tested

specimens, near failure the load reach the maximum value and after this value the load decreased up to 70% to 50% of the maximum load with increasing the descending part of load displacement curves. This indicates the increases of the service load which represent the safe line in using the structures as shown in Table 3 and Fig.12.

Table 2: Comparison between Failure Loads of test specimens

series	Specimen No.	Reinforcing materials	Experimental Failure Ld (KN)	Load-Carrying Capacity Enhancement (%)
control Series	C1	Control specimen reinforced by 4Φ12mm longitudinal steel bars + 11 Φ6mm	723.85	-------
Series A	C1-A	One layer Expanded mesh +4Φ12mm + 6 Φ 6mm	840.40	16.10
	C2-A	Two layers Expanded mesh +4Φ12mm + 6 Φ 6mm	880.00	21.50
	C3-A	Three layers Expanded mesh +4Φ12mm	951.82	31.40
	C4-A	One layers Expanded mesh+4Φ12mm	800.00	10.50
Series B	C1-B	One welded layer mesh+4Φ12mm + 11 Φ 6mm	743.20	2.70
	C2-B	two welded mesh +4Φ12mm + 6 Φ 6 mm	800.00	10.50
	C3-B	one welded layer mesh +4Φ12mm + 6 Φ 6mm	776.66	7.30
	C4-B	two welded meh+4Φ12mm	780.00	7.70
	C5-B	three welded layers mesh+4Φ12mm	833.00	15.10
	C6-B	Four welded layers mesh +4Φ12 mm	867.00	19.80
Series C	C1-C	One layer gavazia mesh +4Φ12mm + 6 Φ 6mm	780.00	7.70
	C2-C	Two layers fiber glass mesh + 4Φ12mm + 6 Φ 6 mm stirrups	725.00	0.17
	C3-C	Three layers fiber glass mesh + 4Φ12mm + 6 Φ 6mm stirrups.	741.88	2.50
Series D	C1-D	One Exp. mesh +one welded mesh + 4Φ12mm + 6 Φ 6mm	839.77	16.0
	C2-D	Two layers Expanded mesh +one layer welded mesh + 4Φ12 mm + 6 Φ 6mm stirrups.	890.00	22.90
Series E	C1-E	One layer Tensar mesh+ 4Φ12mm + 11 Φ 6 mm	787.50	8.70
	C2-E	One layer Tensar mesh + 4Φ12 mm+ 6 Φ 6mm.	732.87	1.30

3.3 Ductility and energy absorption

Ductility is defined as the ratio between the deformation at 0.8 of ultimate load in the descending part to the deformation at the ultimate load, while the energy absorption is the total area under the load deflection curve. Table 3 shows the energy absorption and progressive increase of energy absorption with volume fraction percentage was observed. For the control specimen C1 the energy absorption recorded 439.5 KN.mm, compared this value with the recorded for different series

it shows good enhancement. For all series the enhancement percentage varies between 6.9% and 141%. The smallest enhancement was at series C which use fiber glass instead of stirrups due to the weak properties of the used type of fiber but the highest enhancement was series D which used both expanded and welded wire mesh. As shown in Table 3 and Fig. 13.

For the obtained ductility as shown in table 4 and Fig. 14 the ductility obtained for the control specimen was 1.22. A progressive increase in ductility obtained for different series of specimens. For series A, the ductility varied between 2.13 to 2.67 with an increase of 74.6% to 118.8%. For series B the ductility varied between 1.86 for C6-B to 2.83 for C5-B with an enhancement varied between 52.5% to 132.0%. For series C, the obtained ductility was 1.48, 2.48 and 2.88 for C1-C, C2-C and C3-C with an enhancement of 21.3%, 103.3% and 136.1% respectively. For series D the obtained ductility were 1.93 and 2.61 for C1-D and C2-D with an enhancement of 58.2% and 113.9%. The last series E the ductility for C1-E was 2.54 with enhancement of 108.2% and 2.38 for C2-E with an enhancement of 95.1%. It can be concluded that using these innovative composites enhanced the behaviour of failure by increasing the ductility ratio. Finally using these innovative composite materials enhanced the behavior of the tested columns. It can be state that it delayed the appearance of the first cracks and increased the service load capacity. In addition, it developed with high ultimate loads, crack resistance, better deformation characteristics, high durability, high ductility and energy absorption properties, which are very useful for dynamic applications.

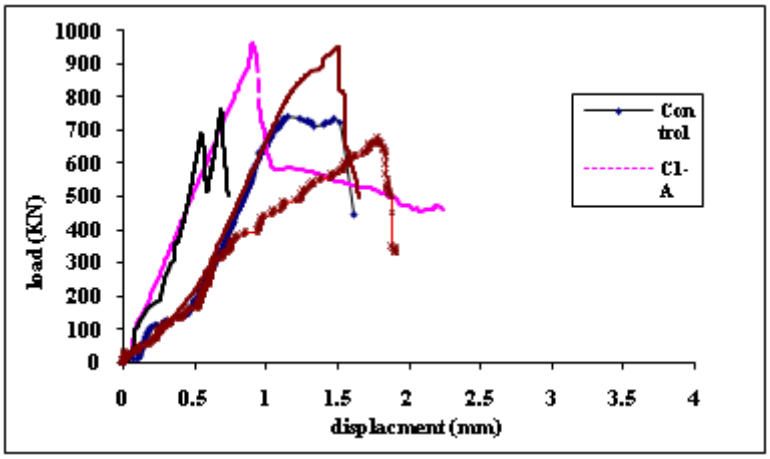

Fig.4: Comparison between Load Displacement Curve of Series A

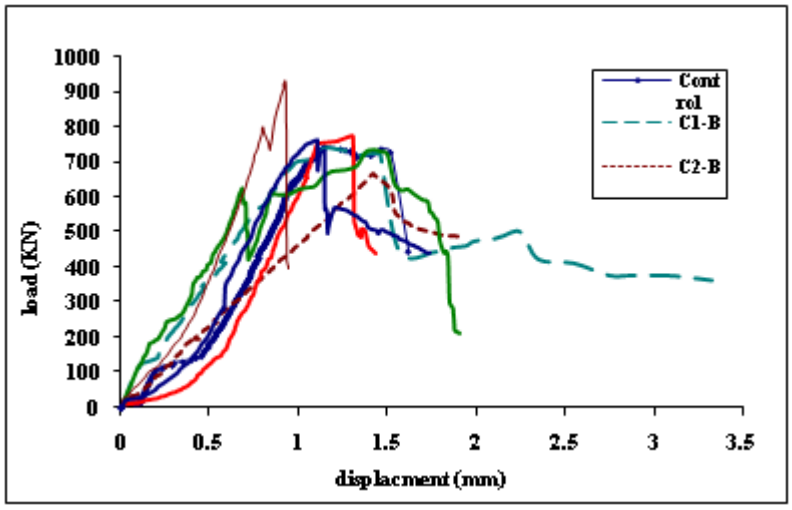

Fig.5: Comparison between Load Displacement Curve of Series B

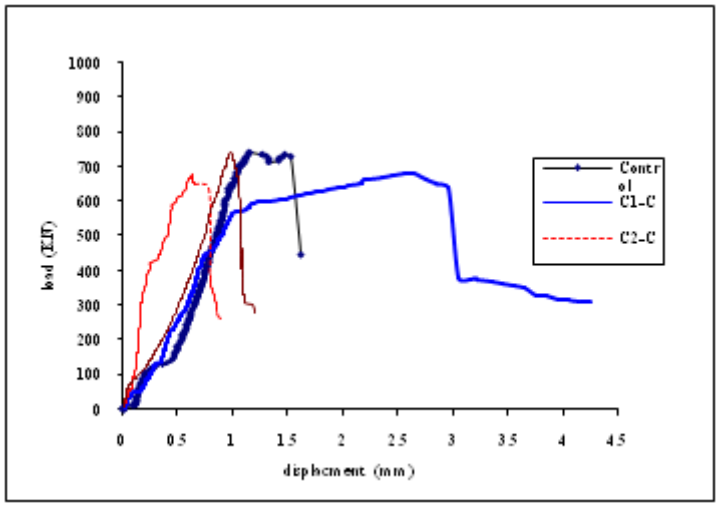

Fig.6: Comparison between Load Displacement Curve of Series C

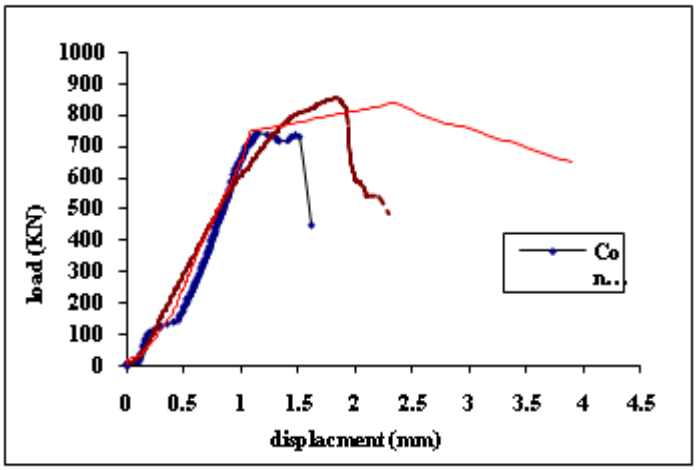

Fig.7: Comparison between Load Displacement Curve of Series D

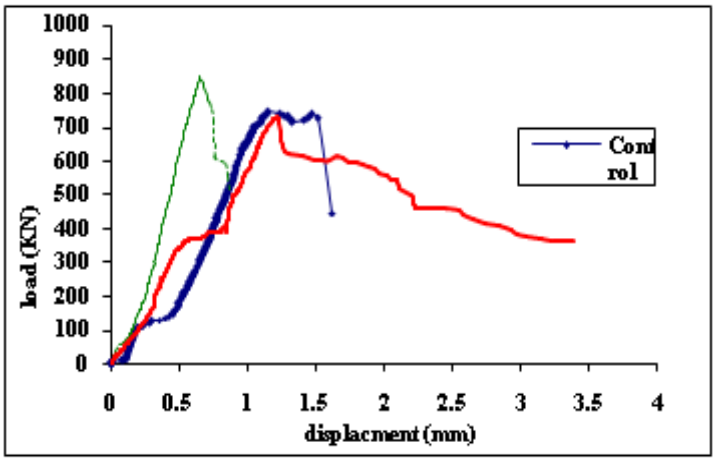

Fig.8: Comparison between Load Displacement Curve of Series E

Table 3: Deformation characteristics of tested columns

	Specimen ID	$P_{F.C}$ (KN)	$\Delta_{F.C}$ (mm)	P_{ser} (KN) Eq.4.1	P_{Umax} (KN) (Test)	ΔP_{Umax}	$(\Delta P_{Umax} / \Delta_{F.C})$	Energy Absorption, KN.mm	% of Energy Absorption enhancement
Control and Series (A)	C1	400	0.846	451.69	723.85	1.55	1.832	439.5	---------
	C1-A	650	0.658	524.54	840.40	1.10	1.671	738.9	68.10
	C2-A	670	0.485	549.29	880.00	0.75	1.546	747.6	70.10
	C3-A	690	0.870	594.18	951.82	1.30	1.494	750.0	70.60
	C4-A	600	1.100	499.29	800.00	1.60	1.454	826.0	87.90
Series B	C1-B	550	0.742	463.79	743.20	1.40	1.886	901.5	105.1
	C2-B	560	0.845	499.29	800.00	1.30	1.538	993.0	125.9
	C3-B	460	0.896	484.70	776.66	1.35	1.506	986.8	124.5
	C4-B	450	0.352	486.79	780.00	0.85	2.414	875.0	99.10
	C5-B	490	0.628	519.92	833.00	1.15	1.831	951.0	116.3
	C6-B	505	0.669	541.17	867.00	1.45	2.167	961.1	118.7
Series C	C1-C	490	0.875	486.79	780.00	2.50	2.857	1042.5	137.2
	C2-C	480	0.883	452.40	725.00	1.65	1.868	470.6	6.90
	C3-C	485	0.717	462.97	741.88	1.25	1.743	530.4	20.68
Series D	C1-D	590	0.839	524.15	839.77	1.60	1.907	1021.7	132.5
	C2-D	600	0.634	555.54	890.00	1.30	2.050	1062.5	141.8
Series E	C1-E	390	0.387	491.48	787.50	0.65	1.679	562.5	27.87
	C2-E	370	0.660	457.34	732.87	1.30	1.951	699.4	59.13

Table 4: Calculation of ductility ratio of tested specimens

Series	**Specimen ID**	**Δ 0.8 P_{Umax} (mm) (Experimental)**	**ΔP_{Umax} (mm) (Experimental)**	**Ductility (Δ 0.8 P_{Umax} / ΔP_{Umax})**	**%of increase in ductility**
Control and Series (A)	C1	1.9	1.55	1.22	------
	C1-A	2.40	1.10	2.18	78.7
	C2-A	1.90	0.75	2.53	107.3
	C3-A	2.95	1.30	2.67	118.8
	C4-A	3.40	1.60	2.13	74.6
Series (B)	C1-B	3.50	1.40	2.50	104.9
	C2-B	3.25	1.30	2.50	104.9
	C3-B	3.20	1.35	2.37	94.3
	C4-B	2.20	0.85	2.59	112.3
	C5-B	3.25	1.15	2.83	132.0
	C6-B	2.70	1.45	1.86	52.5
Series (C)	C1-C	3.70	2.50	1.48	21.3
	C2-C	4.10	1.65	2.48	103.3
	C3-C	3.60	1.25	2.88	136.1
Series (D)	C1-D	3.10	1.60	1.93	58.2
	C2-D	3.40	1.30	2.61	113.9
Series (E)	C1-E	1.65	0.65	2.54	108.2
	C2-E	3.10	1.30	2.38	95.1

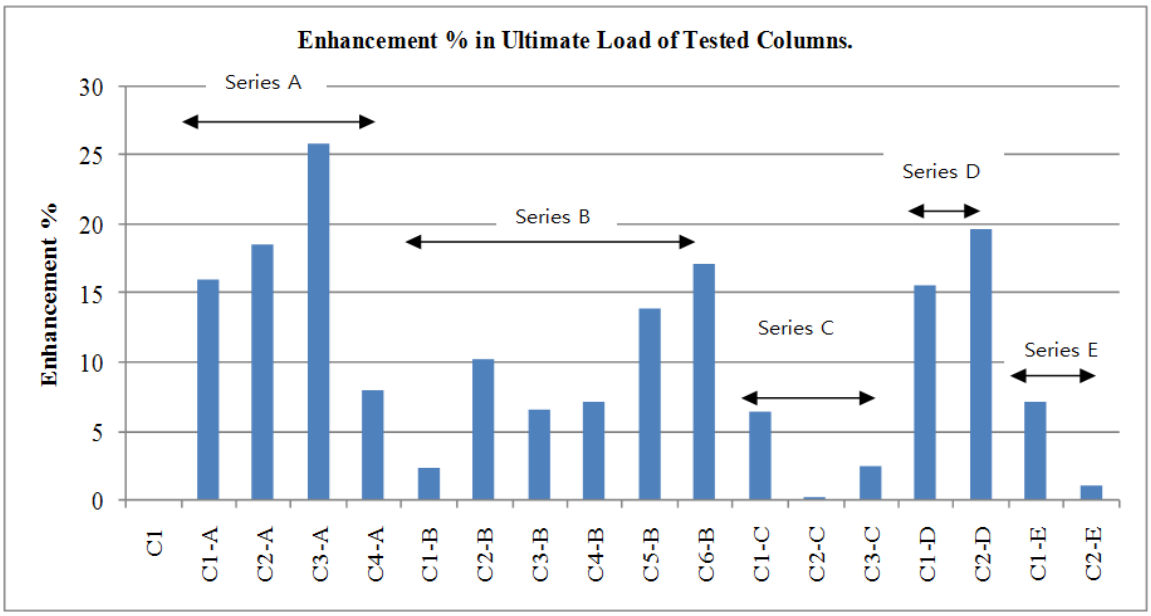

Fig. 9: Enhancement percentage in experimental carrying capacity

a) C1 b) C1-A c) C2-A d) C3-A e) C4-A

Fig. 10 a): cracking pattern; a) C1; b) C1-A ; c) C2-A ; d) C3-A; e) C4-A

1) C1-B 2)C2-B 3)C3-B 4)C4-B 5) C5-B 6) C6-B

Fig. 10 b): cracking pattern; 1) C1-B; 2) C2-B; 3) C3-B; 4) C4-B; 5) C5-B; 6) C6-B

1) C1-C 2) C2-C 3) C3-C

Fig. 10.c): Cracking pattern; 1) C1-C; 2) C2-C; 3) C3-C

1) C1-D 2) C2-D 3) C1-E 4) C2-E

Fig. 10. d): cracking pattern; 1) C1-D; 2) C2-D; 3) C1-E; 4) C2-E

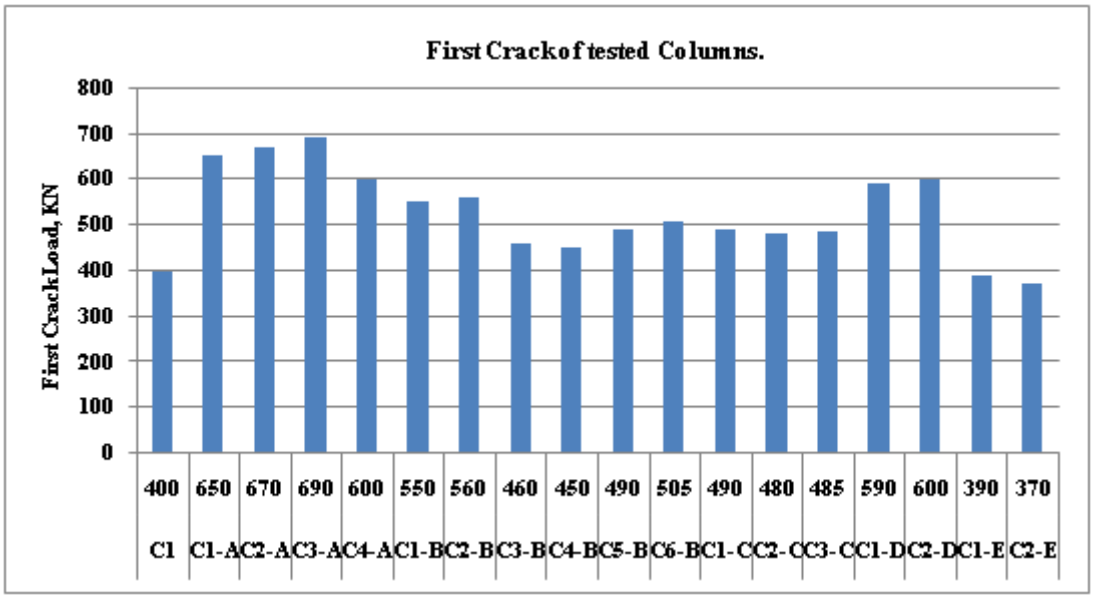

Fig. 11: Comparison between first crack loads of tested columns

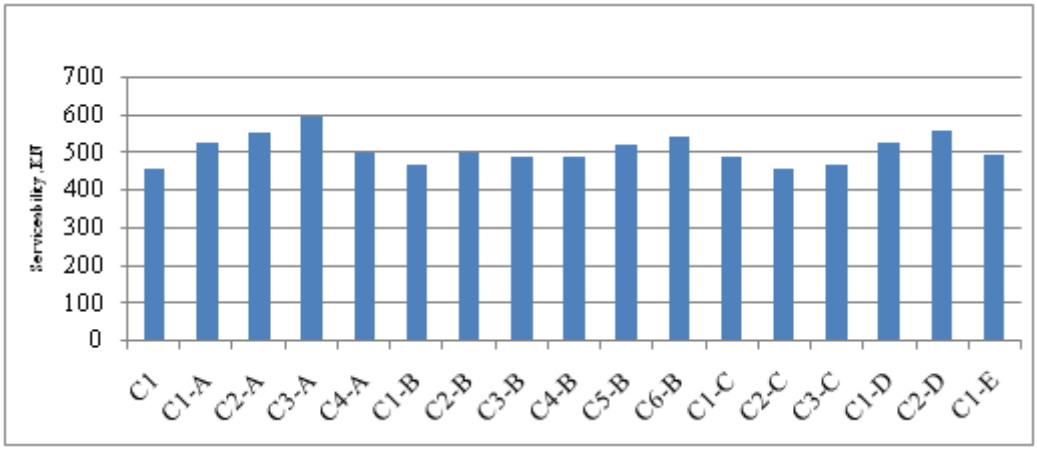

Fig.12: Comparison between serviceability loads of tested columns

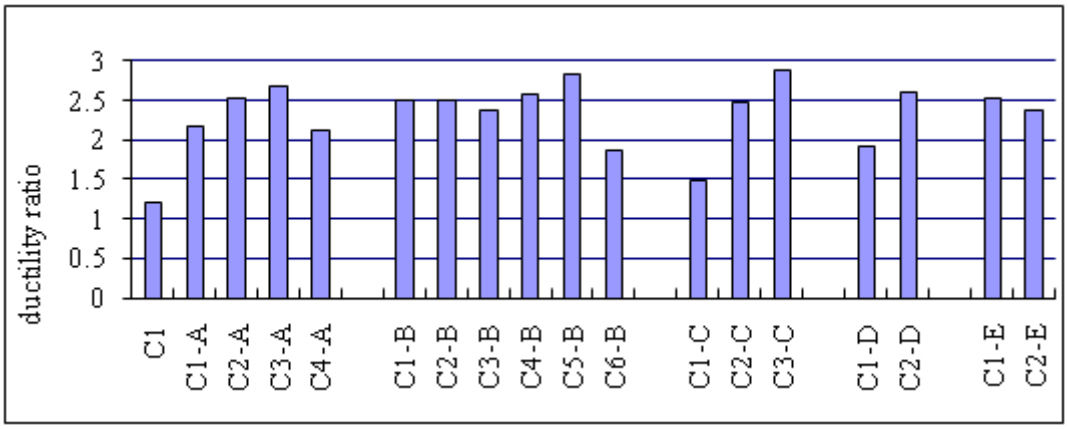

Fig. 13: Comparison between ductility ratios of tested columns

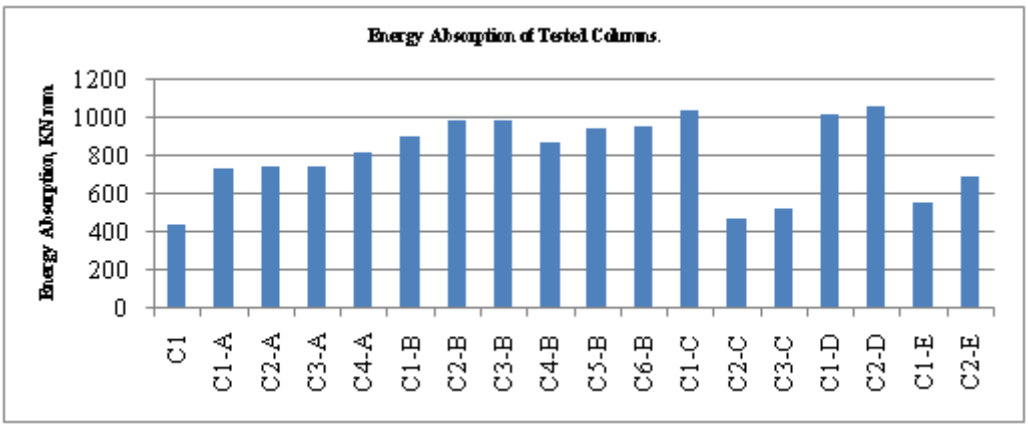

Fig. 14: Comparison between energy absorption of tested columns

4. NON-LINEAR ANALYSIS OF TEST SPECIMENS

Non-linear finite element analysis; (NLFEA) was carried out to investigate the behaviour of the reinforced concrete columns using innovative composites specimens employing ANSYS-9.0 Software [12]. The investigated behaviour includes the cracks pattern, the ultimate load and the load-deflection response of the test specimens. In addition, extensive non linear finite elements analyses had been conducted to investigate in deep the behaviour of the concrete columns reinforced by innovative composites.

4.1. Modelling of Reinforced Concrete Columns

3-D finite elements analysis was conducted for the reinforcing concrete columns with innovative composites. ANSYS-9.0 has several three-dimensional elements in its library; namely Solid45, Solid64, Solid65, and Solid95. In this study, SOLID65 for the concrete as it is suitable for presentation of compression stress-strain curve for concrete other properties. The reinforcing steel bars were modelled using LINK8 3-D element. Also the other innovative composites materials were represented by calculating its volumetric ratio in concrete element using its special properties. The numerical solution scheme adopted for non-linear analysis was an incremental load procedure**.**

4.2 Cracking Behaviour

The cracking was initiated at early loading stage in the concrete elements modelling the loaded face of the column nearby the supporting of columns as shown in Fig. 15 Referring to Table 3, the cracking capacity is shown to be 362.5 KN for all the specimens being independent on the reinforcing characteristics. This early stage of crack loading is due to the unseen micro cracks in experimental test. The cracking load, as such, is quite below the experimental cracking capacity. The ratio of the analytical cracking load to the experimental load. $P_{cr\ (NLFE)} / P_{cr\ (EXP.)}$ is shown to be ranged from 0.53 to 0.97 with a mean value of 0.7. This is may be justified as the NLFE predictions represent the micro-cracking stage which precedes the visible cracking stage. Moreover, the innovative composites materials might have concealed the micro cracks developed underneath in the experiments.

On the other hand, the cracking patterns at each load increment revealed that propagation of the cracks for all specimens was slightly different with respect to the experimental crack pattern. This is due to the accuracy of the non linear finite element program in determined the micro cracks and wide cracks, and reflected the significance of the reinforcing method on the cracking patterns as shown in Table 5.

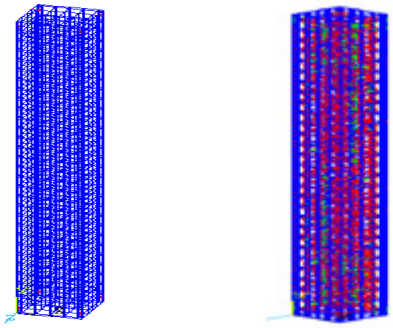

a) b)

Fig. 15: a) First cracks of control specimen, b) all cracks of control specimen." Model-1

4.3 Ultimate load carrying capacity

Good agreement between the NLFEA predictions and the recorded load-carrying capacity is shown in Fig. 5.11 for the control specimen and the analytical ultimate load to the experimental load; $P_{u\ (NLFE)} / P_{u\ (EXP.)}$ was equals to 1.11. For specimens in series A, B, C, D and E the ratio of the analytical ultimate load to the experimental load; $P_{u\ (NLFE)} / P_{u\ (EXP.)}$ ranges between 0.85 and 1.16 with a mean value of 1.05, refer to Table 3 for the result. Furthermore, the analysis reflected the strengthening significance. The analytical enhancement in ultimate load capacity p_u was as the following: For series A the enhancement was 2.7%, 3.9%, 0% and decrease of 0.6% for Specimens C1-A, C2-A, C3-A and C4-A, respectively, against test enhancement of 16.1%, 21.5%, 31.4% and 10.5%, respectively. For series B the enhancement was 6.7%, 3.9%, 5.5%, 3.7%, 2.7% and 2.8% for C1-B, C2-B, C3-B, C4-B, C5-B and C6-B respectively against experimental enhancement of 2.7%, 10.5%, 7.3%, 7.7%, 15.1% and 19.8% respectively. For series C the analytical enhancement for C1-

C, C2-C, and C3-C was 6.7%, 3.9% and 6.1% against to 7.7%, -1.9% and 2.55% experimental increase but for C2-C there was same value in failure load experimentally. For series D the enhancement was 10.1% and 12.7% for C1-D and C2-D, but the experimental enhancement was 16.0% and 22.9%. Finally series E the analytical enhancement was 3.9% for C1-E but for C2-E there was a decrease of 3.3% against to experimental enhancement of 8.7% for C1-E and 1.3% for C2-E. See Fig. 16 to Fig. 5.17.

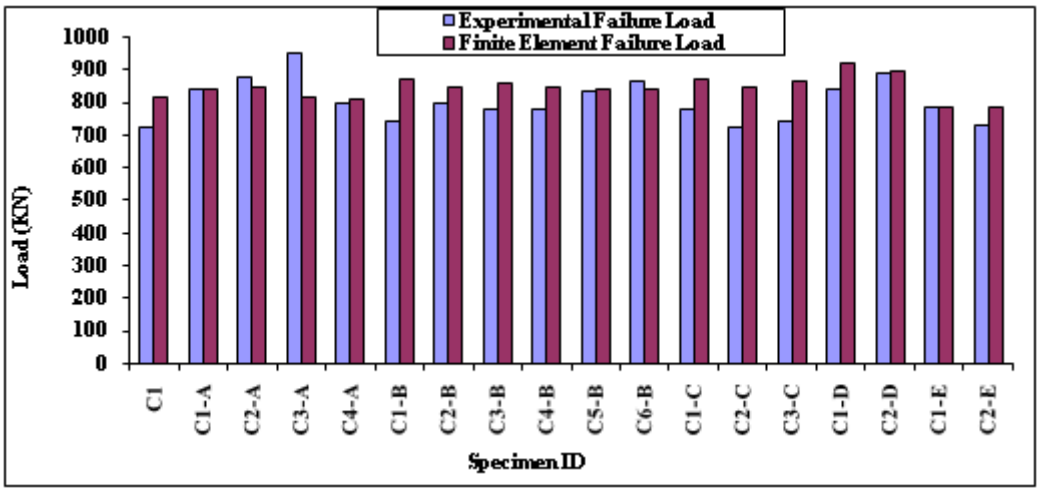

Fig. 16: Comparison between Experimental and Analytical Failure load

Table 5: Comparisons between Finite Element and Experimental

series	Specimen No.	Initiation of cracking; P_{ucr} (KN)		Ultimate Load P_u (KN)		$P_{ucr(NLFEA)}/P_{ucr(EXP)}$	$P_{U(NLFEA)}/P_{u(EXP)}$
		EXP.	NLFEA	EXP.	NLFEA		
Series Control	C1	400	362.5	723.85	815	0.90	1.11
Series A	C1-A	650	362.5	840.4	837.5	0.56	1.0
	C2-A	670	362.5	880	847.5	0.54	0.96
	C3-A	690	362.5	951.82	815	0.53	0.85
	C4-A	600	362.5	800	810	0.60	1.01
Series B	C1-B	550	362.5	743.2	870	0.66	1.16
	C2-B	560	362.5	800	847.5	0.65	1.06
	C3-B	460	362.5	776.66	860	0.79	1.11
	C4-B	450	362.5	780	845	0.81	1.08
	C5-B	490	362.5	833	837.5	0.74	1.01
	C6-B	505	362.5	867	837.79	0.72	0.97
Series C	C1-C	490	362.5	780	870	0.74	1.11
	C2-C	480	362.5	725	847	0.76	1.16
	C3-C	485	362.5	741.88	865	0.75	1.16
Series D	C1-D	590	362.5	839.77	897.5	0.61	1.06
	C2-D	600	362.5	890	918.7	0.60	1.03
Series E	C1-E	390	362.5	787.5	847.5	0.93	1.07
	C2-E	370	362.5	732.87	787.5	0.98	1.02
Average						0.70	1.05

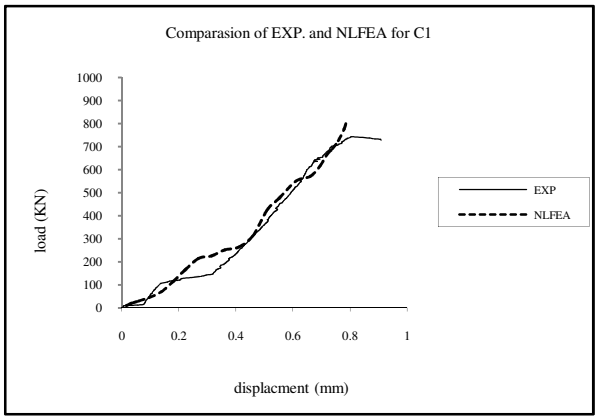

Fig. 17: Comparison between EXP and NLFEA load-displacement curve for C1

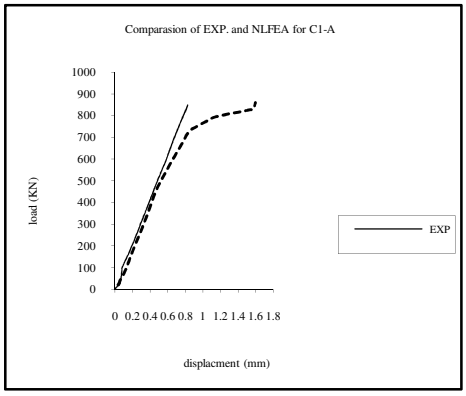

a) C1-A

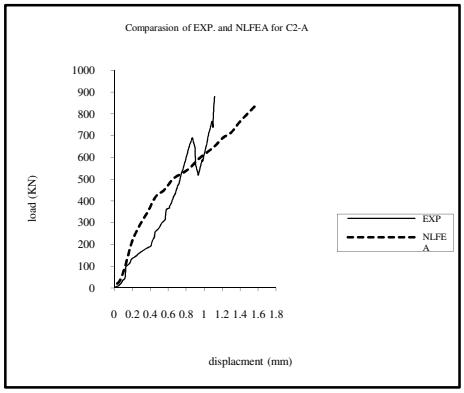

b) C2-A

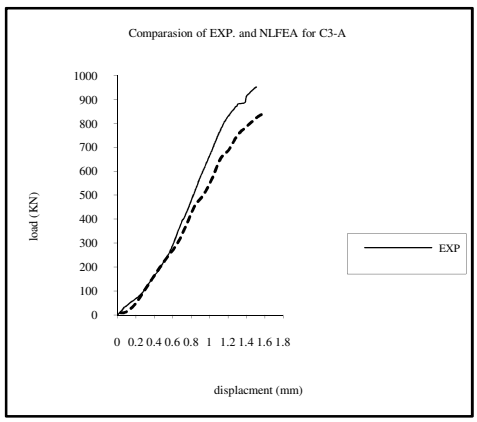

c) C3-A

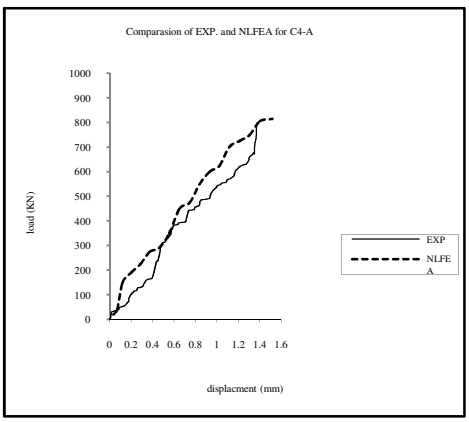

d) C4-A

Fig. 18: Comparison between EXP. and NLFEA load-displacement curves for series A; a) C1-A; b) C2-A;c) C3-A; d)C4-A

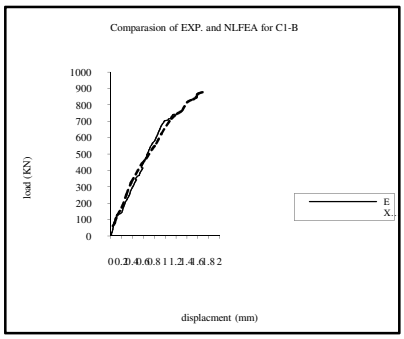

a) C1-B

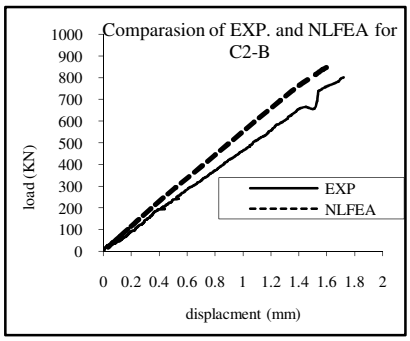

b) C2-B

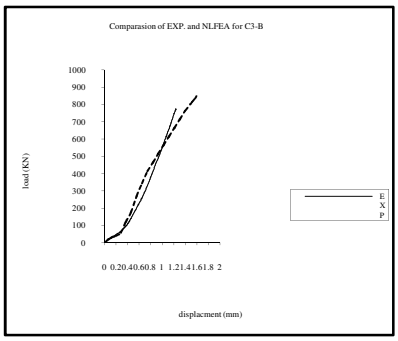

c) C3-B

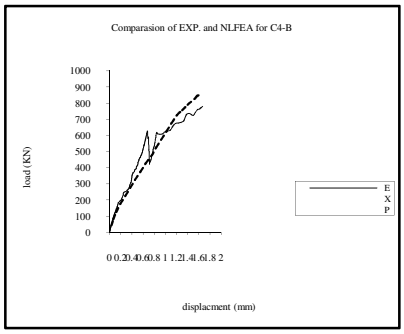

d) C4-B

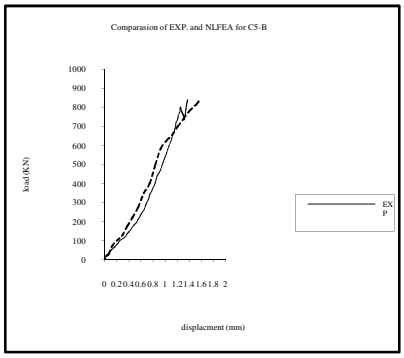

e) C5-B

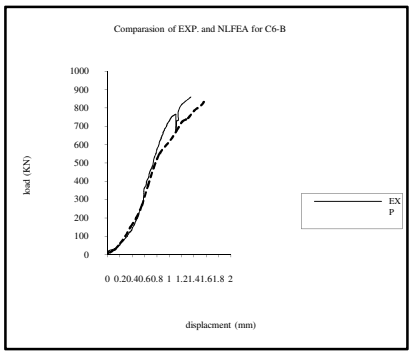

f) C6-B

Fig..19 Comparison between EXP. and NLFEA load-displacement curve for series B a) C1-B, b) C2-B;c) C3-B; d)C4-B; e) C5-B; f) C6-B

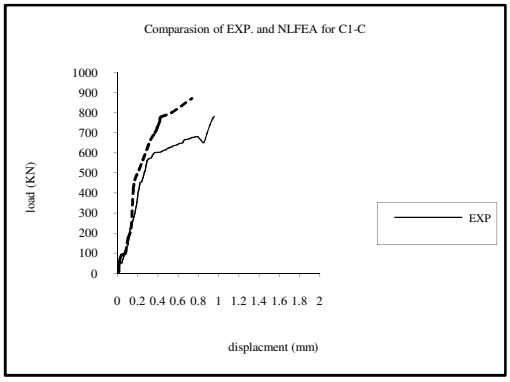

a) C1-C)

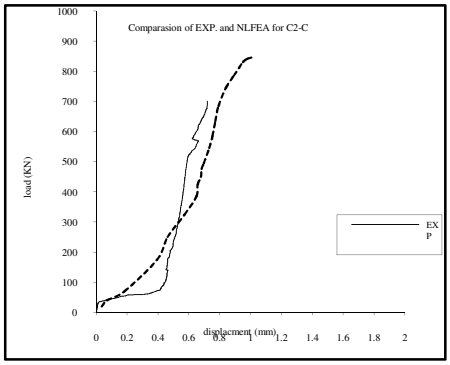

b) C2-C

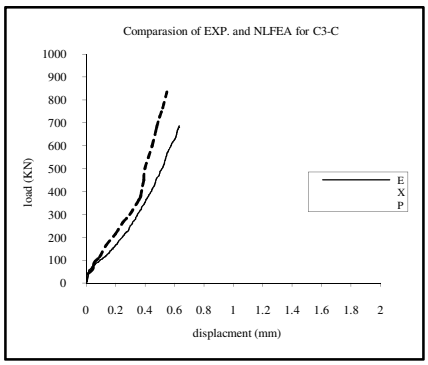

C) C3-C

Fig. 20: Comparison between EXP. and NLFEA load-displacement curve for series C
a) C1-C, b) C2-C, c) C3-C

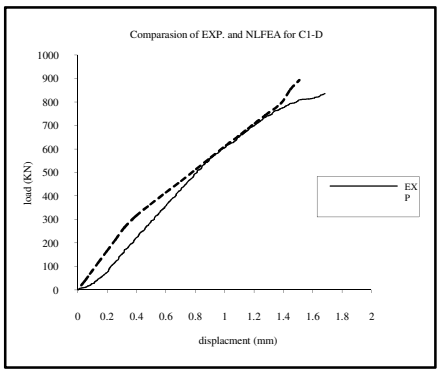

a) C1-D

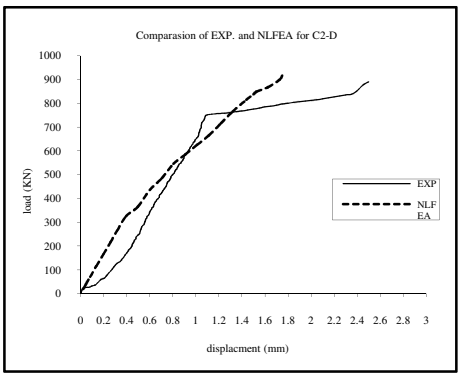

b) C2-D

Fig. 21: Comparison between EXP. and NLFEA load-displacement curve for series D
a) C1-D, b) C2-D

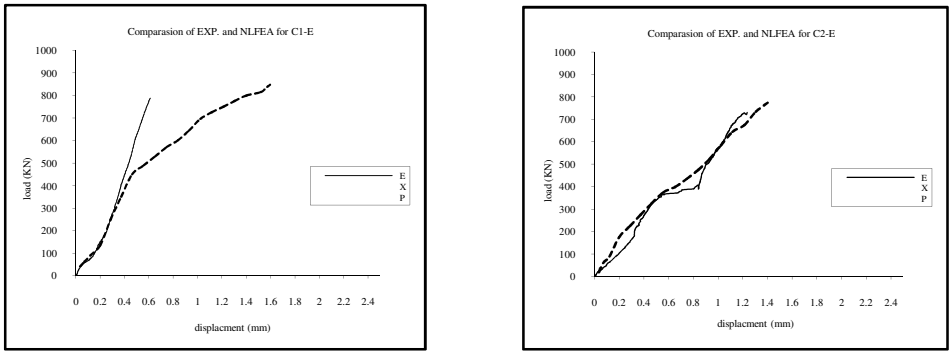

a) C1-E b) C2-E

Fig. 22: Comparison between EXP. and NLFEA load-displacement curve for series E; a) C1-E, b) C2-E

5. CONCLUSIONS

Based on the results and observations of the experimental and the analytical study presented in this thesis and considering the relatively high variability and the statistical pattern of data, the following conclusions can be drawn:

- Irrespective of the steel mesh type, expanded or welded volume fraction of steel reinforcement, ferro-cement specimens tested under axial compression loadings exhibit superior ultimate loads compared to the control ones.

- Increasing in the volume fraction does not have much effect under axial compression loading in which the failure load is mainly governed by the spalling of the mortar cover around the steel reinforcement.

- Changing steel mesh types, expanded or welded have much effect on ultimate loads under axial compression loading. There is higher strength gain of specimens reinforced with welded steel mesh about 32% compared with those reinforced with welded steel mesh.

- The test results show that the welded wire mesh exhibited a higher ultimate load than conventionally reinforced control columns by about 19.8 %, .Column C6-B which was reinforced with four layers of welded steel mesh. Therefore there is strength gain about 20 % by employing galvanized welded steel mesh as reinforcement.

- Comparing the results of ultimate load in case of column C1-C which was reinforced with one layer of gavazzia mesh, which reached 8% higher ultimate load compared to that of control column C1.

- Superior high ultimate load and strength gain could be obtained by using two layers of expanded steel mesh and one layer of welded steel mesh, column C2-D reached 23% compared to that of control column C1.

- Column C1-E which was reinforced with one layer of tensar mesh and 4ϕ12mm steel bars and 11ϕ6mm stirrups exhibited 9% higher ultimate load compared with that of control column C1 without spalling of concrete cover this is predominant.

- Experimental results revealed that increasing the volume fraction of steel reinforcement contributed to a slightly higher ultimate load and higher energy absorption. This is clear when comparing column C2-D which reinforced with 2 layers of expanded steel mesh + 1 layer of welded steel mesh and 4 ϕ 12mm and6 ϕ 6mm stirrups.23% higher strength gain and 66% higher energy absorption compared to that of control C1.

- Therefore increasing volume fraction percentage has a dominant effect in delaying occurrence of the developed cracks with high protection against corrosion and high strength gain compared with those reinforced with metallic reinforcement.

- Innovative columns reinforced with various types of metallic and non-metallic materials were developed with high ultimate loads, crack resistance, better deformation characteristics, high durability, high ductility and energy absorption properties, which are very useful for dynamic applications.

- There is a good agreement between experimental results and theoretical ones, this could be attributed that carefully under taken experimental program was carried out and could be helpful for further parametric studies including various parameters could be investigated.

6. REFERENCES

[1] Mansur. M.N., and Paramasivam, P. (1990), "Ferro-cement Short Columns under Axial and Eccentric Compression", *ACI structural Journal*, 84 (5): 523.

[2] Ahmed T.; Ali S.K. S.; and Choudhury, J.R. (1994), "Experimental Study of Ferro-cement as a Retrofit Material for Masonry Columns", *In Proceedings of the Fifth International Symposium on Ferrcement, Nedwell and Swamy (eds)*, 269-276, London: E& FN Spon.

[3] Kaushik S.K.; Prakash A.; and Singh K.K. (1994), "Inelastic Buckling of Ferro-cement Encased Columns", *In Proceedings of the Fifth International Symposium on Ferrcement, Nedwell and Swamy (eds),* 327-341, London: E& FN Spon.

[4] Nedwell P.J.; Ramesht M.H.; and Rafei-Taghanaki S. (1994), "Investigation into the Repair of Short Square Columns using Ferro-cement", *In Proceedings of the Fifth International Symposium on Ferrcement, Nedwell and Swamy (eds),* 277-285, London: E& FN Spon.

[5] Fahmy, E., Shaheen, Y.B.; and Korany, Y. (1999), "Repairing Reinforced Concrete Columns Using Ferro-cement Laminates", *Journal of ferro-cement* 29(2):115-124

[6] Fahmy, E.H., Shaheen, Y.B.I., and Korany, Y.S. (1999), "Environmentally Friendly High Strength Concrete", *Proceedings of the 24th Conference on Our World in Concrete and Structures,*171-178.

[7] Fahmy, E.H., Shaheen, Y.B., Abou Zeid, M.N., and Gaafar, H. (2004), "Ferro-cement Sandwich and Cored Panels for Floor and Wall Construction", *Proceedings of the 29th Conference on Our World in Concrete and Structures,* 245-252.

[8] Fahmy, E.H., Shaheen, Y.B., & Abou Zeid, M.N. (2004),"Development of Ferro-cement Panels for Floor and Wall construction", *5th Structural Specialty Conference of the Canadian Society for Civil Engineering*, ST218-1-ST218-10.

[9] Fahmy, E.H., Abou Zeid, M.N., Shaheen, Y.B., & Gaafar, H. (2005),"Behavior of Ferro-cement Panels Under Axial and Flexural Loadings", *Proceedings of the 33rd Annual General Conference of the Canadian Society of Civil Engineering*, GC-150-1-GC-150-10.

[10] Abdel Tawab, Alaa, (2006), "Development of permanent formwork for beams using ferro-cement laminates", P.H.D. Thesis, submitted to Menoufia University, Egypt.

[11] Hazem, R.(2009)" Non-metallic Reinforcement for the U-shaped ferro-cement forms instead of the conventional steel mesh ", *Deutsches Zentrum für Entwicklungstechnologien*. Retrieved on February 20.

[12] Fahmy, Yousry B. I. Shaheen, Ezzat H, Ahmed Mahdy Abdelnaby and Mohamed N. Abou Zeid (2013) "Applying the Ferro-cement Concept in Construction of Concrete Beams Incorporating Reinforced Mortar Permanent Forms"; *International Journal of Concrete Structures and Materials*, March 26, accepted November 27, 2013

[13] ANSYS," Engineering Analysis system user's Manual" 2005, vol. 1&2, and theoretical manual. Revision 8.0, Swanson analysis system inc., Houston, Pennsylvania.

[14] Sidramappa Shivashankar Dharane, Madhkar Ambadas Sul and Patil Raobahdur Yashwant, "Earthquake Resistant RCC and Ferrocement Cicular Columns with Main Spiral Reinforcement", *International Journal of Civil Engineering & Technology (IJCIET)*, Volume 5, Issue 9, 2014, pp. 100 - 102, ISSN Print: 0976 – 6308, ISSN Online: 0976 – 6316.